

## Numerical Investigation of Gas Turbine Combustion Chamber Flows

Waheed S. Mohammed,\* Shakair H. Aljanabe,\* Mokdad H. Rahman\*\*

Received on 28/1/2004

Accepted on 18/4/2005

### Abstract

The paper present mathematical model for two-dimensional axi-symmetric, swirling recirculating, elliptic., turbulent, and reacting flow inside annular combustor. The present model is restricted to single-phase, kinetically influenced combustion with negligible radiation heat transfer. the mathematical model comprises differential equation for : Continuity, momentum, stagnation enthalpy, concentration, turbulence energy . wall function approach is incorporated to this model to simulate the boundary near wall region. The simultaneous solution of these equations by means of a finite-difference solution algorithm yields the values of the variable at all internal grid nodes. All procedure is based on development of a computer program in annular combustor. The predicted results indicate that the inlet temperature have significant effect on the performance of flow field. The numerical result shows good agreement behavior of all properties of flow field.

Keywords: CFD, Combustion, turbine flow.

الاستنباط العددي لجريانات غرفة الاحتراق لتوربين غازي

الخلاصة

لقد تم في هذا البحث تقديم نموذج رياضي لجريان ثنائي البعد مضطرب متفاعل داخل محرك حلقي لتوربين غازي . إن نوع التفاعل المستخدم في هذا البحث هو أحادي الطور مع إهمال تأثير انتقال الحرارة. كذلك تم في هذا البحث الاعتماد على معادلات الزخم، الطاقة، الاستمرارية في حل هذا النموذج وتم الأخذ بنظر الاعتبار أيضا تأثير مخلفات التفاعل وتأثير طاقة الاضطراب. دالة الجدار أخذت بنظر الاعتبار أيضا لتمثيل الطبقة المتاخمة واستخدمت طريقة الفروق المحددة في حل هذه المعادلات بالاعتماد على تقسيم مجال الجريان إلى شبكة داخلية دقيقة. تمت خطوات الحل بواسطة تطوير برنامج حاسوبي معد لهذا الغرض. أظهرت النتائج المستوحاة من هذا النموذج الرياضي أنه لدرجة حرارة الدخول تأثير مباشر على أداء الجريان داخل المحرك الحلقي وإن سلوك الجريان داخل المحرك هو سلوك منطقي ومقبول وكذلك تم إظهار نتائج بنية خصائص الجريان داخل المحرك.

### 1. INTRODUCTION

The modeling of a gas turbine combustor should include flow fields , heat transfer, turbulence, and combustion phenomena. These are conjugating different complex processes related to physics (fluid mechanics and transport) and

chemistry .The modeling should also account for sudden expansion of mixture of air and fuel at inlet , the chemistry of combustion of liquid fuel in air, the flow field characteristics of the mixture [1]. The flow field computation in gas turbine combustor is based on the techniques for the

\* Asst.Prof./Al-Rasheed College, UOT.

\*\*Ministry of Sciences and Technology

solution of the elliptic partial equation together with the finite – rate chemical kinetics. The combustion may be considered single phase diffusion controlled. By examining the behavior of velocity, pressure, temperature and chemical composition at points throughout the flow, the mathematical models of gas turbine combustor consist of a set of simultaneous partial differential equations with additional relation for the state variables. Further expression for the rate of production of various quantities are required. For example the production of chemical species may be determined from the law of mass fraction unitizing appropriate thermodynamic and reaction rate data [2].

Computational fluid dynamic (CFD) has attained significant advancements in accurately predicting turbulent flows by means of improved modeling capabilities and higher order numerical techniques. In presence of reacting flows, design and parametric optimizations of combustion system components (injectors, burns, liners, combusts, etc) pose highly difficult challenges, and still have to rely on extensive, and expensive, performance testing [3].

There are two main requisites for a correct evaluation of CFD models, the availability of a set of experimental data accurate and detailed enough to enable the specification of the boundary condition, and a comparison between experimental and numerical information and limitations of the numerical models, simplification have

to be made for specification of the boundary condition and their effects assessed prior of CFD appraisal. To facilitate this and because no correct prediction of combusting flow is possible without a preliminary evaluation of the physical model embedded in the computer codes under less demanding condition, the study of noncombusting gas turbine combustor flow becomes task of great importance in this route toward a greater reliability and confidence of the numerical models and their use in combustor design [4].

## 2- Problem Dependent

Before describing the problem – dependent, the problem embodied in the present work is described. The geometry of the problem is shown in figure (1). A premixed fuel – air mixture is admitted steadily into axi – symmetrical combustion chamber having three dilution hole of diameter 10 mm is at the top wall of combustion chamber. The dilution hole into the chamber is at a distance of 90 mm and the second at 135 mm while the third is at 200 mm. The combustion chamber walls are cylindrical having 80 mm internal diameter and 350 mm length. The set of differential equations for  $\phi$  solved are  $u, v, v_\theta, p', m_{f_0}, f, k, \epsilon,$  and  $h$ . Quantities obtained from auxiliary relations are,  $T, m_{ox}, \mu_{eff},$  and  $\rho$ .

### 2-1 The finite – difference grid and integration domain.

The finite – domain grid employed here exhibits 40 \*20 grid nodes in the  $x$  and  $r$  direction respectively. The

distribution of the grid node is revealed in figure (2). The grid spacing in the radial direction is regular except near axis of symmetry, and spacing in the axial direction is regular from side wall until the third dilution hole and then changed smoothly to minimize the deterioration of the formal accuracy of the finite difference scheme due to variable grid spacing and in such way that a higher concentration of nodes occurs near the hole. A cylindrical polar system of coordinates with the longitudinal direction aligned with the axis of the combustor is used, the annulus is not included, and the hemispherical head and the dilution holes are approximated by rectangular shape.

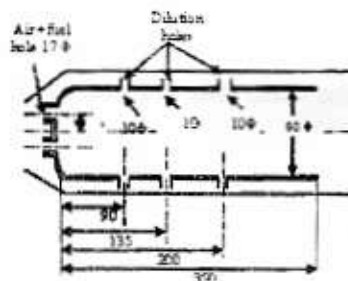


Figure (1) Configuration of combustion chamber  
All dimension in mm



Figure (2) Grid distribution

### 3- Prediction Procedure

#### 3.1 The physical models:

Two main physical models are employed; namely a hydrodynamic

turbulence model, and a combustion model

#### 3.1.1 The hydrodynamic turbulence model

Several models of turbulence have been put forward by different authors. These models differ in complexity and range of applicability; they also involve the solution of different numbers of differential equations. The turbulence model incorporated into this research is the high Reynolds number  $k-\epsilon$  two equations model of Harlow and Nakayama [5] as developed by Lander and Spalding [6]. This model requires the solution of two differential equations, for the two turbulence properties: the kinetic energy of turbulence  $k$ , and its dissipation rate  $\epsilon$ . The model is moderate in complexity. It has been extensively used by many investigators and has proved to be adequate over a wide range of flow situations.

#### 3.1.2 The combustion model

During combustion the fuel (mixture of hydrocarbons) reacts with oxidant stream (air) to form products of combustion. The products are not usually formed in single chemical reaction; the fuel components and the oxidant undergo a series reaction [7].

The combustion model employed here is a relatively simple chemically reacting system (SCRS), which assumes instantaneous reaction with allowance for concentration fluctuations. The instantaneous-reaction assumption implies that whenever fuel and oxidant exist together at a point, chemical reaction

will proceed instantaneously to completion in single step, and producing complete combustion products. As a consequence of this assumption, fuel and oxidant may not present in the same place at the same time. However, because the flow is turbulent, the concentrations of fuel and oxygen fluctuate with time so that at the same point, fuel and oxygen may be present separately, at different times. Thus, the local fluctuation of the concentrations will affect the local time – mean values of unburned fuel mass fraction, and hence the rate of reaction, consequently, an estimate of the magnitude of the fluctuation and its effect on the rate of reaction is required [1].

The rate of the chemical reaction for turbulent flows by an **Arrhenius expression** for laminar flows and by the **eddy – break – up model** for turbulent flows

**3.2 Governing Differential equation**

The mathematical formulation of the flows and the physical models underlying the formulation, are presented in this section. That includes the partial differential equations (PDES), that describe the fluid flow. These equations are based on the conservation of mass (for fuel and matter), momentum, and thermal energy equation. To demonstrate the effect of turbulence on the flow, a turbulence model which involves the solution of two transport equation for the turbulent kinetic energy, **k** and its dissipation rate **ε**, will be described. The mathematical model contains some remarks about additional equation required to

complete the formulation the. General form of the governing differential equation, which can be, expressed all the (PDES) used in mathematical model.

$$\frac{\partial(\beta)}{\partial t} + \frac{\partial}{\partial x}(\beta u \phi) + \frac{1}{r} \frac{\partial}{\partial r}(r \beta v \phi) - \frac{\partial}{\partial x} \left( \Gamma_{\phi} \frac{\partial \phi}{\partial x} \right) - \frac{1}{r} \frac{\partial}{\partial r} \left( r \Gamma_{\phi} \frac{\partial \phi}{\partial r} \right) = S_{\phi} \dots\dots(1)$$

In the above equation  $\phi$  identifies the dependent variable,  $\beta$  is identically equal to either the mixture density  $\rho$  or zero,  $\Gamma_{\phi}$  is the appropriate exchange coefficient for the variable  $\phi$  and  $S_{\phi}$  is the source term which includes both the sources of  $\phi$  (positive or negative) and any other terms which cannot find a place on the left – hand side of the equation. Table (1) summarizes the equations in the form that are solved in present work.

where  $\mu_t = C_D \frac{\rho k^2}{E} \dots\dots\dots(2)$

$$\mu_{eff} = \mu_t + \mu_l \dots\dots\dots(3)$$

is in the table equation **G<sub>k</sub>** is the generation term for the kinetic energy of turbulence and given by :

$$G_k = \mu_t \left\{ 2 \left[ \left( \frac{\partial u}{\partial x} \right)^2 + \left( \frac{\partial v}{\partial r} \right)^2 + \left( \frac{v}{r} \right)^2 \right] + \left( \frac{\partial v_{\theta}}{\partial x} \right)^2 + \left( \frac{\partial u}{\partial r} + \frac{\partial v}{\partial x} \right)^2 + \left( \frac{\partial v_{\theta}}{\partial r} - \frac{v_{\theta}}{r} \right)^2 \right\} \dots\dots(4)$$

where  $\mu_l$  is the laminar or molecular viscosity of the fluid. Often  $\mu_t$  is very large compared with  $\mu_l$  and



$\mu_{eff}$  can be taken equal to  $\mu_t$  without introducing serious errors. This practice is employed in the present work. Recommended values [9] for the constant appearing in the above equations are:

$$C_D=0.09, \quad C_1=1.43$$

$$C_2=1.92,$$

$$\sigma_{k,eff} = 0.9$$

The Schmidt number  $\sigma_{\epsilon,eff}$  for the dissipation rate of turbulence is calculated from:

$$\sigma_{\epsilon,eff} = \frac{\kappa^2}{(C_2 - C_1)\sqrt{C_D}} \dots\dots\dots(5)$$

where  $\kappa$  is the Von-Karman constant. A value of  $\kappa=0.41$  assumed for  $\kappa$  [9].

$\phi$	$\beta$	$\Gamma_\phi$	$S_\phi$
1	$\rho$	0.0	0.0
U	$\rho$	$\mu$	$-\frac{\partial p}{\partial x} + \frac{\partial}{\partial x}(\mu \frac{\partial u}{\partial x}) - \frac{\partial}{\partial r}(\mu_r \frac{\partial u}{\partial r})$
v	$\rho$	$\mu$	$-\frac{\partial p}{\partial r} + \frac{\partial}{\partial r}(\mu \frac{\partial v}{\partial r}) + \frac{1}{r} \frac{\partial}{\partial r}(\mu_r \frac{\partial v}{\partial r}) - \frac{2uv}{r} + \frac{\partial^2 v}{\partial r^2}$
$\omega_\theta$	$\rho$	$\mu$	$-\frac{2}{r} \frac{\partial}{\partial r}(\mu r \omega_\theta)$
k	$\rho$	$\frac{\mu_{eff}}{\sigma_{k,eff}}$	$G_k - \rho \epsilon$
$\epsilon$	$\rho$	$\frac{\mu_{eff}}{\sigma_{\epsilon,eff}}$	$(C_1 G_k - C_2 \rho \epsilon) \epsilon / k$
$m_\theta$	$\rho$	$\frac{\mu}{\sigma_{m_\theta}}$	$R_{m_\theta} = -2\mu^2 T^{1/2} m_\theta \omega_\theta \exp(-E/RT)$ $k^{\frac{1}{2}} = m_\theta$ $k^{\frac{1}{2}} = C_\epsilon k \left[ \left( \frac{\partial m_\theta}{\partial x} \right)^2 + \left( \frac{\partial m_\theta}{\partial r} \right)^2 \right]^{\frac{1}{2}}$
f	$\rho$	$\frac{\mu}{\sigma_f}$	0.0
$\bar{h}$	0.0	$\frac{1}{\omega_\theta + S_\theta}$	0.0

Table (1) Governing Differential Equations

The h-equation expresses the conservation of the stagnation enthalpy of the mixture, defined by:

$$h = m_\theta H_\theta = C_p T \dots(6)$$

It is derived from the first law of thermodynamic together with some simplifying assumption ref. [10].

**Special treatment Near Wall**

To avoid the need for detailed calculations in the near-wall regions, algebraic relations are employed for the near wall grid nodes, which have to be spaced at such a distance from the neighboring walls that lie within the so-called logarithmic layer. Such relations are termed wall functions. References [11], and are derived so as to reproduce identically the implications of the "logarithmic profiles," with uniform shear stress prevailing up to the near wall grid node, and generation and dissipation of energy locally in balance.

The velocities in fluid layers parallel to, and immediately adjoining, a wall obey a modified logarithmic law "law of the wall" [11]

$$u^+ = \frac{1}{k} \ln (E y^+) \dots\dots\dots(7)$$

where

$$u^+ = \frac{u_t}{u_T}, \quad y^+ = \frac{\rho}{\mu_j} k^{\frac{1}{2}} C_\beta^{\frac{1}{2}} \delta \dots\dots\dots(8)$$

$u_t$  is the known velocity tangent to wall

$$u_T = \left( \frac{\tau_s}{\rho} \right)^{1/2} \quad \text{where}$$

$\tau_s = \text{wall shear} \dots \dots \dots (9)$

$= \delta$  distance of the wall from the near – by grid nodes

$\kappa, E$  : constants depending on wall roughness

$\kappa$  is the Vonkarman constant = 0.4 and  $E = 9$  for smooth wall

\*The length scale of turbulence, which is linked to  $k$  and  $\mathcal{E}$ , is proportional to the normal distance from the boundary.

\*The diffusion of turbulence kinetic energy normal to such boundaries is zero

**3.3 The Equation of the Auxiliary Variables**

To complete the mathematical formulation, additional equations one required to: -

**3.3.1 The Combustion Variables: -**

Form tables 1 the value of fuel mass fraction and value of Methane fraction can be calculated as follow.

$$f = \left( \frac{\gamma - \gamma_{Ox}}{\gamma_{fu} - \gamma_{Ox}} \right) \dots \dots \dots (10)$$

$$m_{Ox} = \left( m_{fu} - \frac{f - f_{st}}{1 - f_{st}} \right) s \dots \dots \dots (11)$$

Where  $\gamma_{Ox} = \left( \frac{m_{Ox}}{s} \right)_{inlet}$

$$\gamma = m_{fu} - \frac{m_{Ox}}{s} \dots \dots \dots (12)$$

$\gamma_{fu} = (m_{fu})_{inlet}$  S: staichonetric ratio of oxidant to Fuel

**3.3.2 The Thermodynamic Variables: -**

The time means value of the mixture density is determined from[8]:

$$\rho = \frac{M \bar{p}}{RT} \dots \dots \dots (13)$$

where M is calculated from the computed mass fraction

$$C_{p,mix} = m_{fu} C_{p, fu} + (m_{H_2O} + m_{CO_2}) C_{p, H_2O+CO_2} + (1 + m_{fu} - m_{H_2O} - m_{CO_2}) C_{p, N_2+air}$$

Where  $m_{fu}$ ,  $m_{H_2O}$ , and  $m_{CO_2}$  are the mixture fractions of the unburned fuel, water vapor, and carbon dioxide, receptively.

While  $C_{p, fu}, C_{p, CO_2, H_2O}$ , and  $C_{p, N_2, air}$  are the specific heats at constant pressure of: the fuel, of a mixture of CO<sub>2</sub> and H<sub>2</sub>O resulting from stoichiometric combustion of fuel in O<sub>2</sub>, and a mixture of equal masses of N<sub>2</sub> and air, respectively.

Furthermore,  $C_{p, fu}, C_{p, CO_2, H_2O}$ , and  $C_{p, N_2, air}$  are assumed to vary linearly with temperature according to the following relations

$$C_{p, fu} = 1675 + 2.66T \quad J/kg$$

$$C_{p, CO_2, H_2O} = 1310 + 0.368T \quad J/kg$$

$$C_{p, N_2, air} = 948 + 0.1507T \quad J/kg$$

The constants in equations above were optimized so as to produce the best fit for the individual specific heats, over the range of temperature investigated; the reference values of the component specific heat being those reported in reference [ 12].

The time-mean static temperature is derived form:

$$T = \frac{h - m_{fu} H_{fu}}{C_{p,mix}} \dots \dots \dots (14)$$

### 3-4 The Numerical Solution Procedure:

The set of differential equations are first reduced to finite difference equation exhibiting upwind formation of the coefficient ref [13 ], and then solved iteratively by the "SIMPLE" procedure ref [14].A detailed description of the particular solution procedure employed here is presented in ref [15 ].

### **4- Results and Discussion**

Results are obtained numerically and for turbulent reacting flow with and without heat transfer under the conditions illustrated in the forgoing sections where the mixture flow of air and fuel inside gas turbine combustor is burned at a distance near the inlet of the mixture. These results include the flow field and thermal characteristics for, different inlet temperatures to the combustor (634,656,678 K°), different fuel-air ratio (0.02, 0.018, 0.016), and the turbulence quantities for different velocity ratio (0.5,1.0, 1.2 ).

Figures (1-5) present the velocity vector plots, and clearly indicate the similarity in flow behavior for two cases to be studies. The main features of the flow pattern, such as reversal in the primary zone, jet penetration, and the flow acceleration toward the exit of combustor, are clearly indicated in their figures. The behavior of flow in all regions in the combustor that may contain near-stagnant flow provides valuable assistance. From these figures it can be seen that the value of velocity increased when increased  $T_{in}$ , and F/A ratios and it is clear from

the length of the vector arrow and this due to increasing in kinetic energy of the flow. It can be seen form these figure also the value of exit velocity as labeled in figures is suitable for turbine stage when inlet Mach number about 0.3. These figures give a good agreement for the value of velocity from the inlet to exit of the combustor, for example, figure (1) where the input velocity 137 m/s, the exit velocity 561 m/s and these values is reasonable for the performance of gas turbine combustor.

The gas temperature contours are illustrated in figures (6-10). For the two cases to be studied the values of temperature is increased when increasing  $T_{in}$ , F/A ratios, and fuel types. This is because increasing in the energy input to to the flow .For example in figure (6) the contour line number 13, the temperature value is 2547 K° while in figure (7-28), the same contour line number 13, the temperature is 2581 K°. This increasing in field temperature specially in the exit of the combustor is necessary because it gives energy to the flow, but this increasing is limited to permissible value for the turbine blade, and liner wall. Also when increasing F/A ratio to certain limit to satisfied stable, fast combustion, and low pollution. The behavior of field temperature is reasonable everywhere. The fuel rich mixture prevailing in the primary zone of the combustor results in high gas temperature in this zone due to combustion process as the whole heat being added at the entrance. The subsequent admission of air downstream brings the mixture in cooler regions in particular near the

walls. The regions surrounding the axis of symmetry is relatively higher in temperature than that of the wall, but it less than the region near the entrance. It shows gradually decay from axis of symmetry to the wall.

The transport of fuel is illustrated by the contour plots of fuel mass fraction in figures (11,12). Two cases are to be studied, different inlet temperature, and different F/A ratio. Small increasing in fuel mass fraction about 10% by increasing inlet temperature of the mixture and fuel type due to heat addition to the flow without increasing in mass flow of the mixture. The increasing of F/A ratio from 0.016 to 0.02 will increase the value of fuel mass fraction by 15% due to increasing the quantity of fuel which causing uncompleted combustion. Value above 1% occurs only within the primary zone of the combustor. The fuel jet, unable to penetrate the toroidal vortex prevailing in combustor head, mixes with the swirler flow and escape between the primary jets, being transported near the wall with reduced mixing with the central core of the flow, formed mainly by primary jet fluid. In the dilution region, the jets, because of their weaker penetration drive the fuel toward the centerline.

The contour plots in figures (13,14) show the oxygen mass fraction. Three cases are to be studied, different inlet temperature, different F/A ratio, and different fuel type. These figures can easily show that the oxygen mass fraction values above 80 percent in the regions near dilution hole because no fuel. The regions of primary zone and axis of combustor have relatively

lower value due to mixing with the mixture. Small effect of oxygen mass fraction with increasing inlet temperature, and F/A ratio, of the fuel.

Figure (15) shows the turbulent kinetic energy distribution at different velocity ratios ( $U_{in}/U_d$ ). The turbulent kinetic energy peaks at the jets entry and the three dilution holes and then deices rapidly and spreads downstream the region with the jets combined. It is noted that the effect of velocity ratios is very small everywhere except at the entry region and this due to difference in production, transport, and dissipation of kinetic turbulent energy between the three peaks of the entry jets associated with different velocity ratios. Figs. (16), and (17) shows the predicated contours of turbulent viscosity for different  $T_{in}$  and F/A ratio. It is evident for increased  $T_{in}$  and F/A the field turbulent viscosity increased, From these figures it can be seen that the values of viscosity change through the flow field, which increasing in zones of high turbulent kinetic energy and high temperature due combustion of mixture and decreasing with increased of axial distance due to enhance the mixing between entry and dilution ports.

### **5-1 Conclusions:**

Numerical investigation of flow field inside gas turbine combustor is performed. The numerical study is done by solving the governing equations that are based on the conservation of mass fuel and matter, using finite difference technique. Finite domain computer program that



could handle the problem is developed. Two cases are investigated: different inlet temperature, and different F/A ratio. The distribution of velocity, composition variable, eddy viscosity, and other flow property are given in the computation. The main conclusions of this work are: -

1. The effect of velocity ratios is very small everywhere except at the entry region.
2. Increased  $T_{in}$  and F/A will decrease the field turbulent viscosity.
3. The peaks of turbulent kinetic energy of jets decay rapidly and spread with downstream distance in the region when the jets combined.
- 4- The values of viscosity change through the flow field, which increasing in zones of high turbulent kinetic energy and high temperature due combustion of mixture and decreased with increased of axial distance.
- 5- The behavior of flow represented by vector plots in all regions in the combustor provides good agreements.
- 6-The value of velocity increases when increasing  $T_{in}$  and F/A ratios
- 7- The value of exit velocity is suitable for turbine stage when inlet Mach number is about 0.3.
- 8- The behavior of field temperature is reasonable everywhere
- 9- The regions surrounding the axis of symmetry have relatively higher temperature than that of the wall, but it is less than the regions near the entrance.
- 10- The temperature values show gradually decay from axis of symmetry up to the wall.

11- The increasing of F/A ratio will increase the value of fuel mass fraction by 15%. Value above 1% occurs only within the primary zone of the combustor.

12- The oxygen mass fraction values are above 80 percent in the regions near dilution hole.

13- The regions of primary zone and axis of combustor have relatively lower value of oxygen mass fraction.

14- Small effect of oxygen mass fraction with increasing inlet temperature, and F/A ratio

### 5-2 Recommendations:

In this section some proposals are made for improving and extending the present numerical model. These proposals are listed below:

1. Extend the present model to three – dimensional
2. Extend the present study for different entry ports of fuel and oxidant.
3. Using the present model to study two-phase flow combustion.
- 4- Studying the radiation heat transfer.

### **References**

- [1] Christophe Duwig, "Numerical and Experimental Validation of A Gas Turbine Combustor Design for Gasified Biomass Combustion", Licentiate thesis Stockholm Sweden, 2000.
- [2] Jou, James Riley J., "Progress in Direct Numerical Simulation of Turbulent Reacting Flows" AIAA Journal vol. 27, No.11, November 1989.
- [3] Duranti S., Traverso S., Pittaluga F., "Numerical Simulation of 3D Reacting Flow in Gas Turbine

Combustors", DIMSET, University of Genova 2000, Via Montallegro 1,16145 Genova-Italy.

[4] McQuirk J.J, Paima L.M. , " The flow inside a Model Gas Turbine Combustor: Calculation". Transactions of the ASME vol. 115, July 1993.

[5] Harlow F.H., Nakayama P.I., "Transport of Turbulent Energy Decay Rate". Los Almos Sci.Lab., University of California LA-3854, February 1968.

[6] Launder B.E., Spalding D.B., " The Numerical Computation of Turbulent Flows". Computer Methods in Applied Mechanics and Engineering, vol 3, PP. 169-289, 1974.

[7] Versteeg H.K., Malalasekera W., "An Introduction to Computational Fluid Dynamics. The Finite Volume Method" Longman Group Ltd. 1995.

[8] Serag-Eldin M.A., and D.B. Spalding "Computations of Three-Dimensioned Gas-Turbine Combustion Chamber Flows" Transaction of the ASME Vol.101, July 1979.

[9] Takuro Makita, and Tomonaga Miyazaki, " Turbulent Combustion Characteristics of A Pressurized Methane -Air Combustor under Fuel-Rich Conditions". IJPGC 2000 - 15048

[10] Spalding, D. B., " Diffrential Equation of a Reaction Continuum," Imperial Collage, Mechanical Engineering Dept., Report ref. RF/TM/A/2, Apr.1971.

[11] Spalding D.B., " Concentration Fluctuation in around Turbulent Free Jet" Chem. Eng. Sic., 26 PP. 98-107,1971.

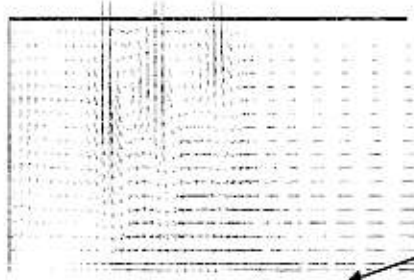
[12] Spiers, H. M., Ed., Technical Data on Fuel, Six Edition Published by the British National Committee Word powered Conference, London, 1962.

[13] Spalding, D. B., " A Novel Finite-Difference Formulation for Differential Expression Involving Both First and Second Derivative "Int. Journal of Numerical Methods in Engineering, Vol. 4, 1972, pp. 551-559.

[14] Caretto and others, " Two Calculation Procedure for Steady-Three- Dimensional Flows With Recirculation," Proceeding of the third Int. Conf. On Numerical Methods in Fluid Mechanics, Vol. II, 1973.

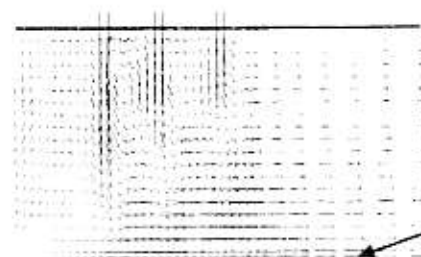
[15] Mokdad H. Abo-Ragheef, " The Numerical and Experimental Investigation of flow field inside Gas Turbine Combustor ", Ph.D. Thesis, University of Technology, Baghdad, Iraq, 2003.

$V_{in}=198\text{ m/s}$   
 $Mach\ No.=0.32$



$Mach\ No.=0.82$

Figure (1) Velocity vector for  $T_{in}=656\text{ K}^\circ$   
and  $F/A=0.02$



$615\text{ m/s}$   
 $Mach\ No.=0.82$

Figure (4) Velocity vector for  $T_{in}=634\text{ K}^\circ$   
and  $F/A=0.018$

$V_{in}=230\text{ m/s}$   
 $Mach\ No.=0.35$



$615\text{ m/s}$   
 $Mach\ No.=0.82$

Figure (2) Velocity vector for  $T_{in}=678\text{ K}^\circ$   
and  $F/A=0.02$

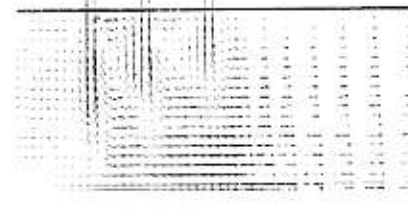
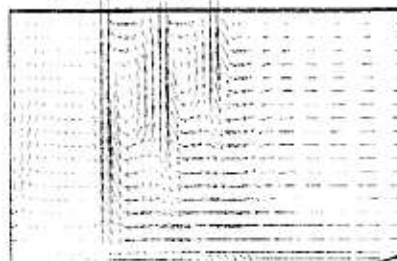


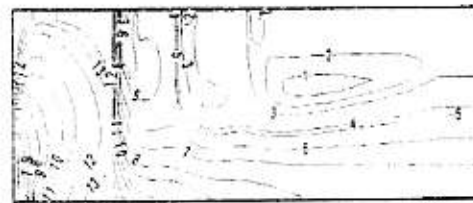
Figure (5) Velocity vector for  $T_{in}=634\text{ K}^\circ$   
 $F/A=0.016$

$V_{in}=255\text{ m/s}$   
 $Mach\ No.=0.38$



$675\text{ m/s}$   
 $Mach\ No.=0.84$

Figure (3) Velocity vector for  $T_{in}=678\text{ K}^\circ$   
and  $F/A=0.02$



14	2579.25
13	2547.46
12	2495.22
11	2363.01
10	2229.81
9	1963.36
8	1696.97
7	1297.34
6	1030.92
5	813.529
4	764.506
3	655.792
2	640.488
1	632.969

Figure (6) Temperature contour for  
 $T_{in}=634\text{ K}^\circ$   $F/A=0.02$

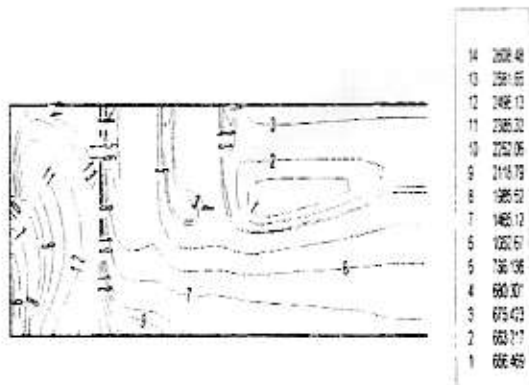
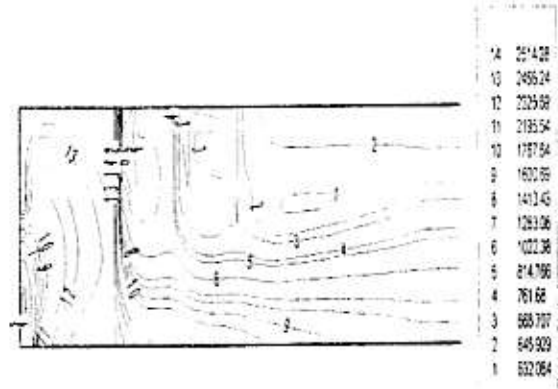


Figure (7) Temperature contour for  $T_{in}=656 K^{\circ}$   
 $F/A=0.02$



Figure(9) Temperature contour for  $T_{in}=634 K^{\circ}$   
 $F/A=0.018$

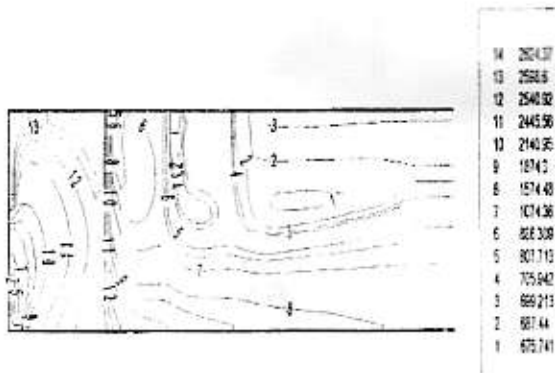
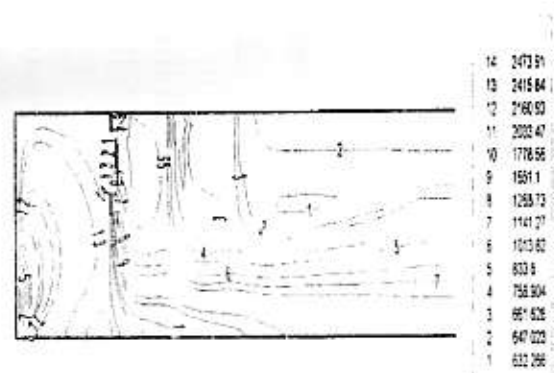


Figure (8) Temperature contour for  $T_{in}=678 K^{\circ}$   
 $F/A=0.02$



Figure(10) Temperature contour for  $T_{in}=634 K^{\circ}$   
 $F/A=0.016$

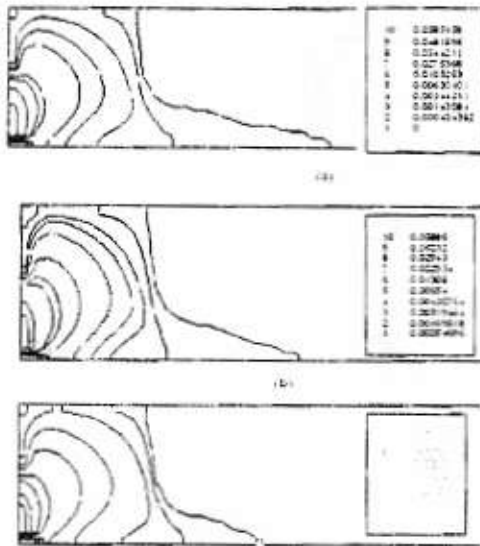


Figure (11) Fuel mass fraction for different  $T_{in}$  (a)  $T_{in} = 634$  K, (b)  $T_{in} = 656$  K (c)  $T_{in} = 678$  K

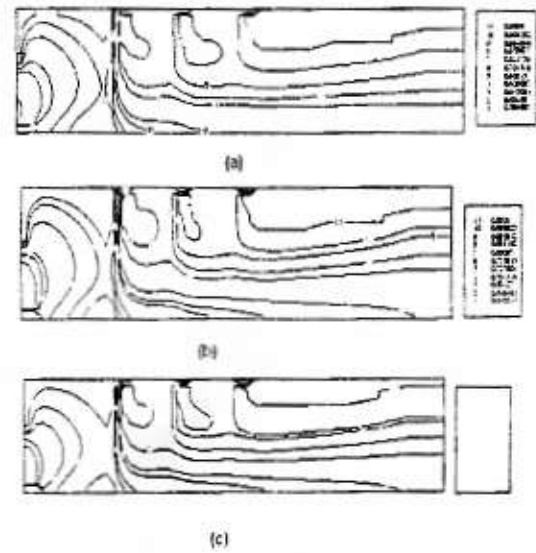


Figure (13) Oxygen mass fraction for different  $T_{in}$  (a)  $T_{in} = 634$  K (b)  $T_{in} = 656$  K (c)  $T_{in} = 678$  K

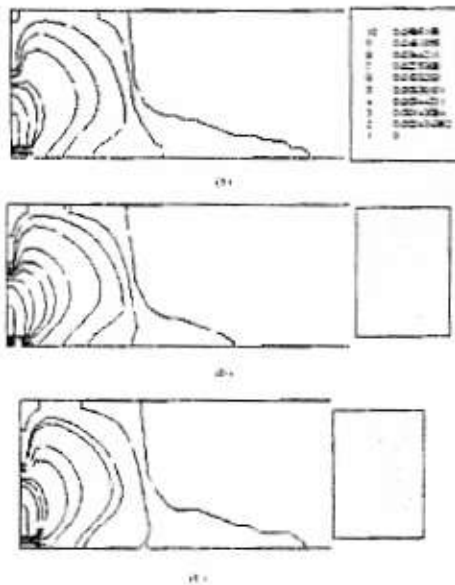
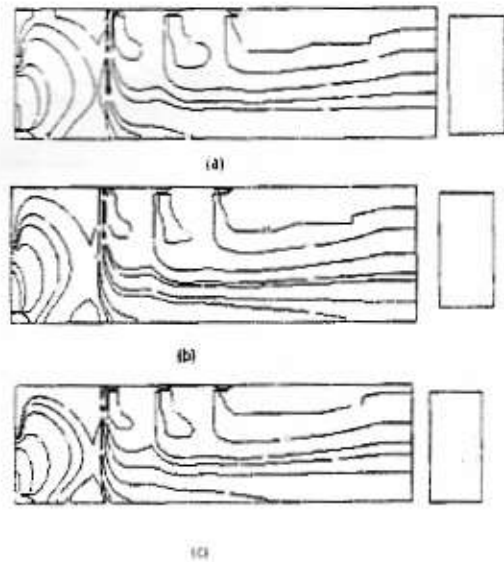


Figure (12) Fuel mass fraction different F/A ratio (a)  $F/A = 0.02$  (b)  $F/A = 0.018$  (c)  $F/A = 0.016$



Figure(14) Oxygen mass fraction for different F/A ratio (a)  $F/A = 0.02$  (b)  $F/A = 0.018$  (c)  $F/A = 0.016$



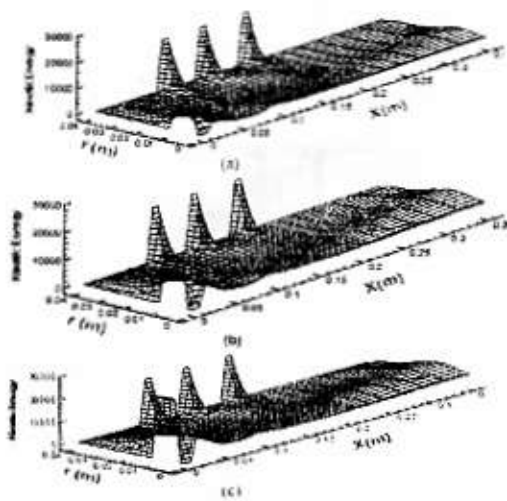


Figure (15) Distribution of kinetic energy (a)  $U_{in}/U_d=0.5$  (b)  $U_{in}/U_d = 1.0$  (c)  $U_{in}/U_d = 1.2$

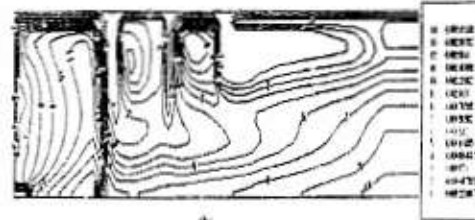
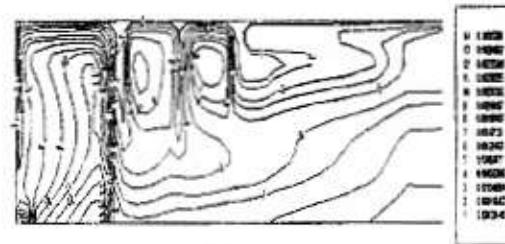


Figure (17) Turbulent for different fuel type

- (a) Kerosene ( $C_8H_{18}$ )
- (b) Ethan ( $C_2H_6$ )
- (c) Methane ( $CH_4$ )

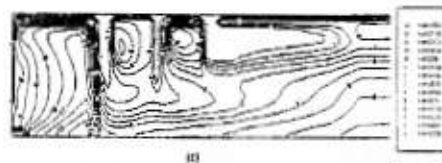
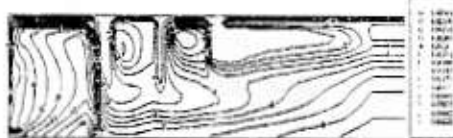


Figure (16) turbulent viscosity for different  $T_{in}$

- (a)  $T_{in} = 634$  K
- (b)  $T_{in} = 656$  K
- (c)  $T_{in} = 678$  K